



HAL
open science

Design Optimization of a New Nanostructured P-GaN Gate for Normally-off GaN HEMTs

Daniel Rouly, Josiane Tasselli, Patrick Austin, Chaymaa Haloui, Karine Isoird, Frédéric Morancho

► **To cite this version:**

Daniel Rouly, Josiane Tasselli, Patrick Austin, Chaymaa Haloui, Karine Isoird, et al.. Design Optimization of a New Nanostructured P-GaN Gate for Normally-off GaN HEMTs. 29th International Conference on Mixed Design of Integrated Circuits and Systems (MIXDES 2022), Jun 2022, Wroclaw, Poland. 10.23919/MIXDES55591.2022.9838389 . hal-03697713

HAL Id: hal-03697713

<https://hal.science/hal-03697713v1>

Submitted on 17 Jun 2022

HAL is a multi-disciplinary open access archive for the deposit and dissemination of scientific research documents, whether they are published or not. The documents may come from teaching and research institutions in France or abroad, or from public or private research centers.

L'archive ouverte pluridisciplinaire **HAL**, est destinée au dépôt et à la diffusion de documents scientifiques de niveau recherche, publiés ou non, émanant des établissements d'enseignement et de recherche français ou étrangers, des laboratoires publics ou privés.

Design Optimization of a New Nanostructured P-GaN Gate for Normally-off GaN HEMTs

Daniel Rouly, Josiane Tasselli, Patrick Austin, Chaymaa Haloui, Karine Isoird, Frédéric Morancho
LAAS-CNRS, Toulouse University, CNRS, UPS
Toulouse, France
drouly@laas.fr

Abstract—A new AlGaIn/GaN heterostructure is proposed to achieve a normally-off behavior for GaN HEMTs. It relies on multiple P-GaN wells epitaxial regrowth along the gate. Simulation results are presented by focusing on the physical and geometrical parameters of the P-GaN wells. The normally-off behavior of the novel HEMT is demonstrated.

Keywords—HEMT; P-GaN gate; normally-off; TCAD simulations

I. INTRODUCTION

AlGaIn/GaN high-electron mobility transistors (HEMTs) have attracted worldwide attention in power electronics as candidates for next-generation of high-speed switching devices. Thanks to the large electric field of GaN and the high carrier mobility and density in the two-dimensional electron gas (2DEG), AlGaIn/GaN HEMTs can achieve high breakdown voltage and realize ultrahigh power density operation with low power losses.

While most of the demonstrated AlGaIn/GaN HEMTs are inherently normally-on with a negative gate threshold voltage, normally-off mode is strongly demanded to fulfill the requirements of power electronics applications; indeed normally-off devices are inherently secure and suitable for energy converters requiring specifically high system reliability. Several approaches, each with its own limitations, have been proposed to convert the inherent depletion mode (normally-on) into an enhancement one (normally-off). The recess of the AlGaIn barrier under the gate (or recessed gate) [1,2], Fluorine plasma ion implantation [3], oxygen treatment [4], gate injection transistor (GIT) [5] and P-GaN gate [6,7] are the most developed ones.

In this paper, we propose a new HEMT structure that combines two of these approaches i.e. recessed and P-GaN regrowth gate. The use of a P-GaN layer on the AlGaIn/GaN heterostructure under the gate contact lifts up the conduction band level, inducing the depletion of the two dimensional electron gas (2DEG) channel, even in the absence of an external bias, thus ensuring the normally-off behavior.

The novelty of our structure relies on the gate conception: it is characterized by the implementation of a succession of P-GaN wells spaced by active AlGaIn/GaN zones along the gate as shown on Fig.1. A lateral depletion effect takes place, allowing the decrease in the 2DEG density on each well sidewall. By acting on the well topology, the 2DEG channel can be fully depleted or not.

Design and optimization of P-GaN wells are described with a focus on the influence of their geometrical parameters (width, depth and spacing) and on the influence of the technological parameters of both the AlGaIn layer (thickness and aluminum content) and the GaN wells (P doping concentration). The simulated electrical transfer characteristics of the novel AlGaIn/GaN HEMT are presented, highlighting the normally-off behavior. In the last section, we report on the technological developments performed for fabricating the nanostructured P-GaN gate HEMT.

II. DEVICE STRUCTURE

A. HEMT description

Fig.1 shows different schematic views of the new AlGaIn/GaN HEMT with multiple P-GaN wells along the gate. Fig. 1a is a 3D view of the whole HEMT. Fig. 1b is a schematic cross section along the gate showing the alternation of P-GaN wells and AlGaIn/GaN active zones. The schematic cross section along the drain-source axis is drawn across a P-GaN well (Fig. 1c) and between two wells (Fig. 1d).

The epitaxial layers parameters used for the simulations are the following: a 20 nm $\text{Al}_{0.2}\text{Ga}_{0.8}\text{N}$ barrier, a 1.7 μm GaN layer, a resistive AlGaIn buffer layer, a 200 nm AlN transition layer on a silicon substrate. The GaN and AlGaIn are considered to be non intentionally doped (NID) at $1 \times 10^{16} \text{ cm}^{-3}$ and $1 \times 10^{15} \text{ cm}^{-3}$ respectively. The gate-source spacing, the gate-drain spacing and the gate length are 1 μm , 5 μm and 300 nm respectively. The source and drain contacts are Schottky ones.

B. Simulated elementary cell description

2D and 3D simulations were performed with SENTAURUS TCAD software. In order to first evaluate the impact of the insertion of P-GaN wells through the layers stacking, we present simulations at the thermodynamic equilibrium. The studied structure being symmetrical and in order to minimize calculation times, we considered only a half cell as described on Fig. 2.

As mentioned in the introduction, the insertion of P-GaN wells along the gate leads to the formation of PN junctions formed by the P-regions and the AlGaIn and GaN active regions neighboring the different well sides: a space charge region (SCR) or depleted zone is naturally created, which extension depends on the wells design. The on-state or off-state behavior of the HEMT is the consequence of the SCR modulation obtained by applying an electrical potential on the P-GaN

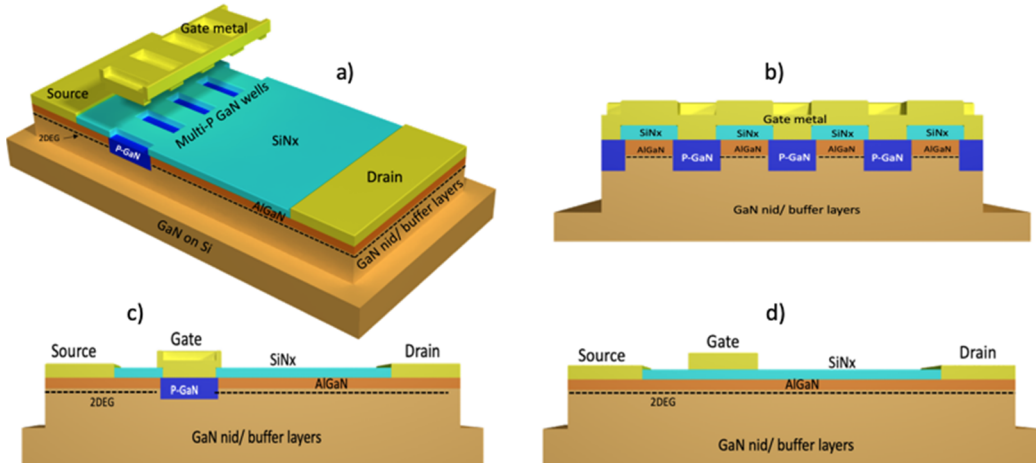


Fig. 1. 3D and cross sectional views of the multi P-GaN wells gate HEMT

regions, i.e. on the gate contact. The major parameters which directly influence on the lateral SCR extension are the following: e_T , L_T and Na respectively the depth, width and doping of the P-GaN wells and D_T the spacing between two wells. We also considered the influence of the Al content of the AlGaIn barrier layer.

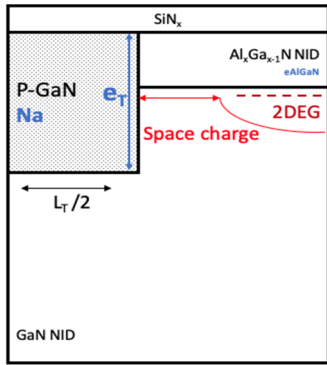


Fig. 2. Schematic cross sectional view of the simulated half cell

III. SIMULATION RESULTS AND DISCUSSIONS

A. Influence of the P-GaN depth e_T

2D simulations have been first performed to evaluate the influence of the well depth on the lateral space charge extension between the P-GaN region and the 2DEG as illustrated on Fig. 3. The P-GaN width L_T is fixed to 100 nm, the AlGaIn layer width to 20 nm, and we varied the doping concentration (Na) of the P-GaN region for two values of the aluminum content of the AlGaIn layer, $x_{Al} = 0.25$ and $x_{Al} = 0.15$.

The results are reported on Fig. 4: the channel depletion width increases with e_T until achieving a maximum value for e_T around 100 nm. This depth value will be retained for the following simulations. The depletion width through the channel also increases with Na , and decreases when the aluminum content increases. For example, for a P doping concentration varying from $1 \times 10^{18} \text{ cm}^{-3}$ to $1 \times 10^{19} \text{ cm}^{-3}$ and x_{Al} fixed to 15%, the depletion width extends from 30 nm to 45 nm respectively.

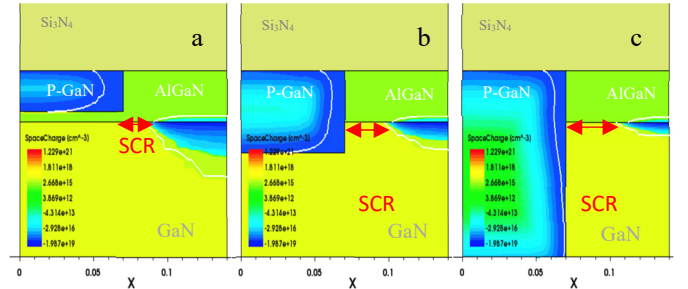


Fig. 3. Example of 2D simulations of the space charge region extension for different P-GaN well depths: a) $e_T = 20$ nm, b) $e_T = 35$ nm, c) $e_T = 100$ nm

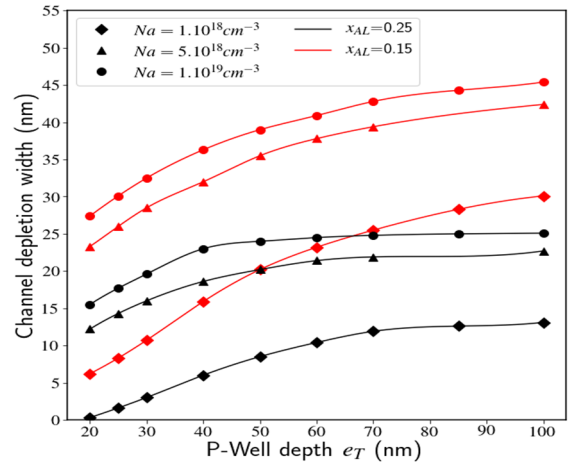


Fig. 4. Simulated channel depletion width variations as a function of the P-GaN well depth, for two aluminum contents (0.25 and 0.15) and different P-GaN doping concentrations ($1 \times 10^{18} \text{ cm}^{-3}$, $2 \times 10^{18} \text{ cm}^{-3}$ and $1 \times 10^{19} \text{ cm}^{-3}$)

B. Influence of the aluminum content x_{Al}

We plotted on Fig. 5 the variations of the lateral depletion width as a function of the polarization charges density at the interface AlGaIn/GaN. Indeed, the 2DEG channel is the result of the piezoelectric and spontaneous polarization charges through these two layers: the higher the aluminum content, the higher the charges density and, as a consequence, the higher the 2DEG

density. To obtain the normally-off functionality for this HEMT, it will be necessary to maximise the lateral depletion width. For an Al content of 20 %, value commonly used, and a P-doping concentration of $1 \times 10^{19} \text{ cm}^{-3}$ e.g., the optimum value of the lateral space charge extension through the 2DEG is 28 nm.

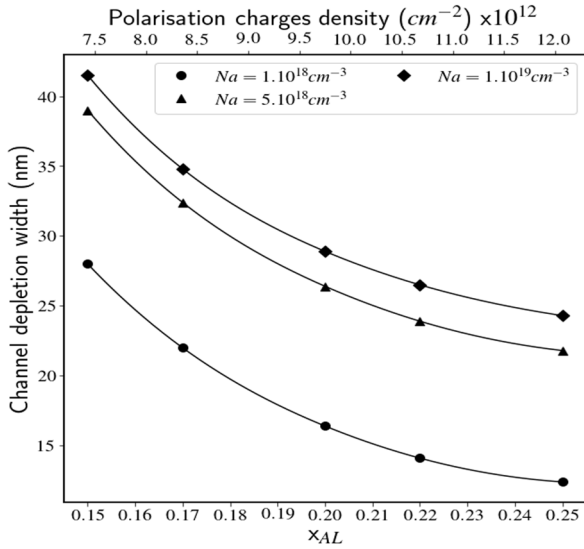


Fig. 5. Simulated variations of the channel depletion width as a function of the aluminum content x_{Al} and the polarisation charges density for different P-doping concentrations

C. Influence of the P-GaN well width L_T

We have also analyzed the impact of the well width L_T on the width of the depleted zone which extends on each side of the P-GaN regions. The behavior can be fitted by an exponential function from which we can extract the minimum value L_{Tmin} of the well width at 95 % of the maximum SCR extension width. In Fig. 6a, it can be seen that the space charge no longer extends from a well width value corresponding to L_{Tmin} .

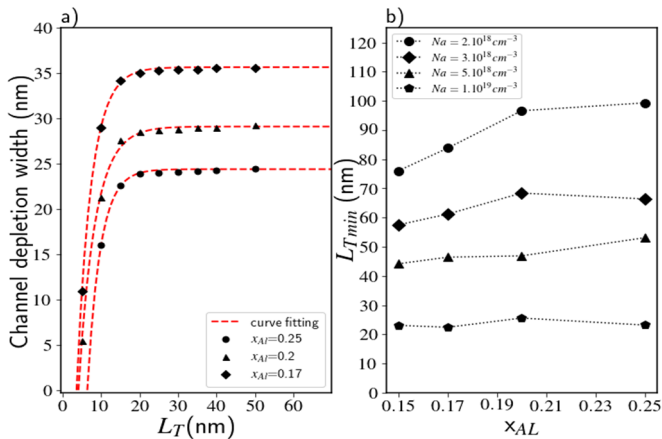


Fig. 6. a) Simulated variations of SCR width as a function of L_T for a $1 \times 10^{19} \text{ cm}^{-3}$ P-GaN doping concentration and different aluminum contents x_{Al} ; b) L_{Tmin} variations as a function of x_{Al} for different P-doping concentrations ($\epsilon_T = 100 \text{ nm}$)

For a $1 \times 10^{19} \text{ cm}^{-3}$ P-GaN doping concentration, the minimum value is 25 nm whatever the aluminum content. We have determined the L_{Tmin} value necessary to achieve a maximum SCR extension, for various P-GaN doping concentrations and Al contents, with a 100 nm well depth (Fig. 6b). For P-doping concentrations higher than $5 \times 10^{18} \text{ cm}^{-3}$, there is a little influence of x_{Al} . For lower doping concentrations, it will be necessary to increase L_T in order to obtain an optimum depletion width.

D. Influence of the well spacing D_T

The geometrical and physical parameters of the P-GaN wells have been optimized to obtain a maximum depletion extension for each one. We consider now a whole cell, comprising two wells spaced by the length D_T . We have determined the spacing necessary to achieve the SCRs overlapping, thus inducing a full channel depletion and obtaining the HEMT's self-blocking.

It is well known that it is necessary to lift the conduction band energy level E_C above the Fermi level to achieve the normally-off functionality for the HEMT by depleting the channel at the AlGaIn/GaN interface. So we have analyzed the evolution of the minimum E_C value extracted at the middle of the channel as a function of two well spacing for different Na doping concentration values (Fig. 7). The minimum energy decreases linearly when D_T increases to reach a threshold when the channel is no more depleted, so rendering the HEMT normally-on. This spacing threshold increases with the P-GaN doping concentration.

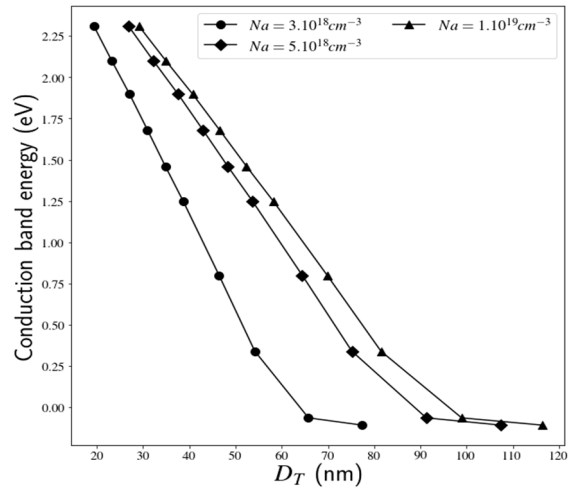


Fig. 7. Simulated variations of the conduction band energy level versus the well spacing D_T for different P-GaN doping concentrations

Considering the conventional P-GaN normally-off HEMTs studied in the literature, the only way to modify the threshold voltage V_{TH} is acting on the P-GaN doping concentration. The novel HEMT structure presented in this paper offers a better flexibility with the advantage to modulate V_{TH} by varying either the P-GaN wells geometrical parameters or their spacing or their doping concentration.

E. On-state behavior of the multi P-GaN well gate HEMT

3D simulations have been performed to observe the on-state behavior of our HEMT structure. The electron mobility in the channel is fixed at $2000 \text{ cm}^2/\text{V.s}$ taking into account the models

of the mobility degradation of the electrons saturation speed at strong electric field. We also considered a Schottky contact on the P-GaN wells. Due to the symmetry of the structure, a half cell is still studied.

The maximum drain saturation current I_{Dmax} and the threshold voltage V_{TH} are extracted from the simulated transfer characteristics $I_D(V_{GS})$ plotted for different channel widths D_T and a drain voltage V_{DS} of 1 V (Fig. 8). The well parameters are the optimum ones defined on the previous simulations, i.e. $L_T = 30$ nm, $e_T = 100$ nm, $x_{Al} = 0.20$ and $N_a = 10^{19}$ cm⁻³. The normally-off behavior of the new HEMT structure is validated with positive threshold voltages. When the channel width increases, V_{TH} decreases as it was expected from previous 2D simulations.

With our structure, we can achieve V_{TH} values higher than those obtained for standard P-GaN HEMTs [8] and FinFET AlGaIn/GaN HEMT topologies regarding the same channel width [9,10]. However, we can see that the maximum current value strongly depends on the channel width, due to the area aspect ratio between the P-GaN and the 2DEG channel regions. The maximum drain current value is around 1 kA.cm⁻² which is a coherent value similar than the ones found in literature [11].

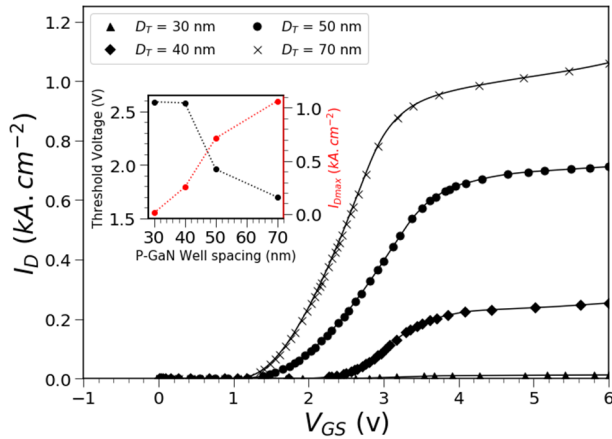


Fig. 8. Simulated transfer characteristics $I_D(V_{GS})$ at $V_{DS} = 1$ V for various D_T with $L_T = 30$ nm, $e_T = 100$ nm, $x_{Al} = 0.20$, $N_a = 1 \times 10^{19}$ cm⁻³, and a Schottky contact on the gate.

IV. TECHNOLOGICAL DEVELOPMENTS

Most of the P-GaN gate HEMT technologies developed are based on the selective GaN layer etching on top of the AlGaIn barrier to define the source and drain access regions. However, the plasma-induced damages may affect the electrical performances of the device due to surface leakage currents. One technology that overcomes these problems and that we have developed in our laboratory consists in fabricating the Mg-doped P-GaN region by selective epitaxy using a SiO₂ growth mask [12,13].

We present in this part the results obtained for a normally-off HEMT that we have fabricated by associating both recess-gate and P-GaN regrowth technics [14-16] with the GaN layer regrown on the whole gate area. The validation of this process led us to develop afterwards the new normally-off HEMT structure presented in this paper with multi P-GaN wells along the gate.

A. Normally-off HEMT with a MBE regrown P-GaN gate

The HEMT structure was characterized by an AlGaIn barrier of 25 nm thick with an aluminum rate of 20 %. At first, a 100 nm thick silicon oxide SiO₂ layer was deposited by PECVD (Plasma Enhanced Vapor Deposition), acting as a mask for both the AlGaIn gate etch and the selectively GaN regrowth. After a CF₄ RIE etch of the SiO₂ layer to define the gate region, a Cl₂ partial etching of the AlGaIn layer was performed by ICPECVD with the following conditions: RF power of 60 W, pressure of 5 mTorr and Cl₂ flow rate of 10 sccm. For an etch time of 35 s, 19 nm of AlGaIn was removed. A 50 nm GaN layer P-doped with Magnesium (Mg) was then regrown in a MBE (Molecular Beam Epitaxy) reactor with a nominal acceptor concentration of Na-Nd of 4×10^{18} cm⁻³.

Figure 9 shows a TEM cross-section view of the gate region with the regrown P-GaN layer on the etched AlGaIn layer. The analysis highlights the perfect nucleation of the GaN layer on the etched AlGaIn layer. The next technological steps concerned the mesa isolation and the gate, source and drain metallisations.

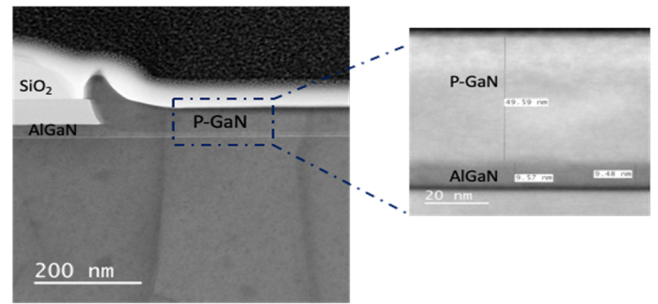


Fig. 9. TEM cross-section view of 50 nm P-GaN layer regrown by MBE on the etched AlGaIn layer.

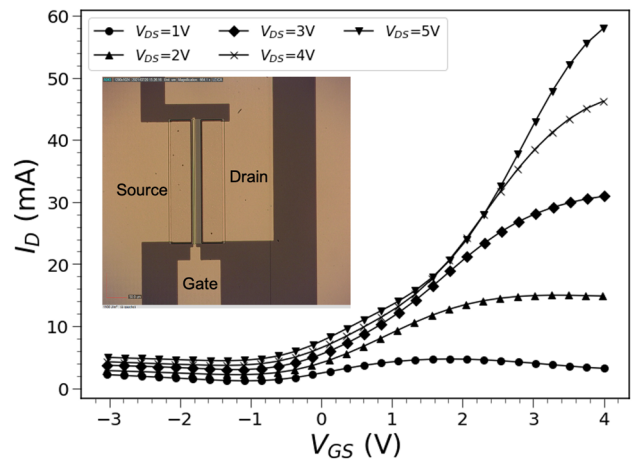


Fig. 10. View of the recessed and regrown P-GaN gate normally-off HEMT developed at LAAS and measured transfer characteristics $I_D(V_{GS})$ for various V_{DS} , with $N_a = 4 \times 10^{18}$ cm⁻³ and a Schottky contact on the P-GaN.

The measured transfer characteristics $I_D(V_{GS})$ of the fabricated HEMT for various V_{DS} values are reported on Fig. 10, for a Schottky contact on the gate. The normally-off behavior was demonstrated with positive threshold voltages around 1 V.

B. Normally-off HEMT with a multi P-GaN wells gate

The fabrication of the novel proposed HEMT structure is in progress. The first technological step we have developed is the e-beam lithography of the 200 nm thick HSQ resist at the nanometric scale in order to define the 50 nm wide active regions separating the different P-GaN regions. Fig.11 shows a MEB view after the lithography of the HSQ lines across the gate, which is delimited by the SiO₂ layer, and the BCl₃ etching of the AlGa_xN/GaN layers with both HSQ and SiO₂ as an etch mask, thus resulting in the formation of the different wells. The next step of the process will be the selective area growth of the P-GaN regions inside the etched wells.

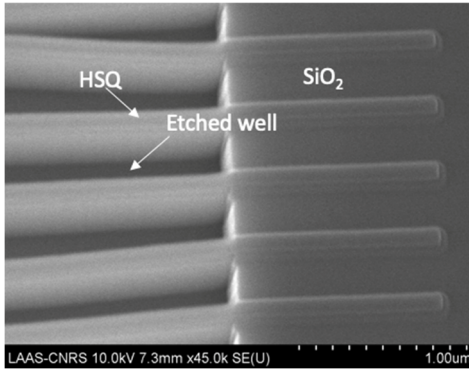


Fig. 11. MEB view of the multiwells along the gate after HSQ e-beam lithography and AlGa_xN/GaN BCl₃ etching.

V. CONCLUSION

A new normally-off AlGa_xN/GaN HEMT structure with multiple P-GaN wells along the gate is proposed in this paper. The P-GaN HEMTs developed up to now necessitate an accurate control of the gate recess with the disadvantage of channel mobility degradation. In our structure, the 2DEG channel properties are maintained between two wells. A lateral space charge region extends on each side of them, thus depleting the adjacent channel created by the AlGa_xN/GaN heterostructure.

2D simulations have highlighted that with an appropriate design of the well i.e. depth, width, spacing between each one, and P-GaN doping concentration, we can obtain the normally-off functionality with a degree of freedom in the choice of the AlGa_xN layer parameters (thickness and aluminum content). The benefit of the proposed HEMT was demonstrated from 3D simulations, positive threshold voltages being achieved. This structure paves the way for the integration of advanced power functions.

The HEMT fabrication is in progress: the critical technological steps such the wells shaping at the nanometric scale and the GaN regions regrowth have been developed.

ACKNOWLEDGMENTS

This work is funded by the IPCEI on Microelectronics research program “Nano2022”. This work was partly supported by LAAS-CNRS Micro and Nanotechnologies Platform, member of the French RENATECH network, and by the calculation platform of LAAS-CNRS.

The authors would like to thank F. VAURETTE from the IEMN Micro and Nano Fabrication Platform for providing HSQ e-beam lithographies and Y. CORDIER and É. FRAYSSINET from CRHEA-CNRS for performing MBE P-GaN epitaxies.

REFERENCES

- [1] J. T. Asubar, S. Kawabata, H. Tokuda, A. Yamamoto, and M. Kuzuhara, “Enhancement-Mode AlGa_xN/GaN MIS-HEMTs with High V_{TH} and High I_{Dmax} Using Recessed-Structure With Regrown AlGa_xN Barrier” *IEEE Electron Device Lett.*, vol. 41, n° 5, p. 693-696, May 2020.
- [2] H. Huang *et al.*, “Design of novel normally-off AlGa_xN/GaN HEMTs with combined gate recess and floating charge structures”, in *2013 IEEE 10th International Conference on Power Electronics and Drive Systems (PEDS)*, Kitakyushu, Apr. 2013, p. 555-558.
- [3] K. J. Chen *et al.*, “Physics of fluorine plasma ion implantation for GaN normally-off HEMT technology,” *2011 International Electron Devices Meeting*, 2011, pp. 19.4.1-19.4.4, doi: 10.1109/IEDM.2011.6131585.
- [4] Y.-L. He *et al.*, “Recessed-gate quasi-enhancement-mode AlGa_xN/GaN high electron mobility transistors with oxygen plasma treatment,” *Chin. Phys. B*, vol. 25, no. 11, p. 117305, Nov. 2016.
- [5] H. Okita *et al.*, “Through recessed and regrowth gate technology for realizing process stability of GaN-GITs,” *2016 28th International Symposium on Power Semiconductor Devices and ICs (ISPSD)*, 2016, pp. 23-26, doi: 10.1109/ISPSD.2016.7520768.
- [6] Y. Zhong *et al.*, “Effect of Thermal Cleaning Prior to p-GaN Gate Regrowth for Normally Off High-Electron-Mobility Transistors”, *ACS Appl. Mater. Interfaces*, vol. 11, no. 24, pp. 21982–21987, Jun. 2019.
- [7] G. Greco, F. Iucolano, et F. Roccaforte, “Review of technology for normally-off HEMTs with p-GaN gate”, *Mater. Sci. Semicond. Process.*, vol. 78, p. 96-106, May 2018.
- [8] H. Jiang *et al.*, « Thin-barrier heterostructures enabled normally-OFF GaN high electron mobility transistors », *Semicond. Sci. Technol.*, vol. 36, n° 3, p. 034001, March 2021.
- [9] M. Zhu *et al.*, « P-GaN Tri-Gate MOS Structure for Normally-Off GaN Power Transistors », *IEEE Electron Device Lett.*, vol. 42, n° 1, p. 82-85, Jan. 2021.
- [10] M. A. Alsharif *et al.*, « Theoretical Investigation of Trigate AlGa_xN/GaN HEMTs », *IEEE Trans. Electron Devices*, vol. 60, n° 10, p. 3335-3341, Oct. 2013.
- [11] H. Guo *et al.*, « 3-D Simulation Study of a Normally-OFF GaN Lateral Multi-Channel JFET With Optimized Electrical Field Transfer Terminal Structure », *IEEE Trans. Electron Devices*, vol. 69, n° 4, p. 1918-1923, Apr. 2022.
- [12] H. Fu *et al.*, « Selective area regrowth and doping for vertical gallium nitride power devices: Materials challenges and recent progress », *Materials Today*, vol. 49, p. 296-323, Oct. 2021.
- [13] G. Rolland *et al.*, “High Power Normally-OFF GaN/AlGa_xN HEMT with Regrown p Type GaN”, *Energies*, 14(19):6098, Sept. 2021.
- [14] M. Charles and G. Toulon, “Normally-off HEMT with high threshold voltage and a low on-state resistance” Patent FR 3 047 609-A1
- [15] C. Haloui, “Development and technological fabrication of GaN HEMT devices with the normally-off functionality”, PhD thesis, Université de Toulouse, July 2021.
- [16] C. Haloui *et al.*, « Recessed and P-GaN regrowth gate development for normally-off AlGa_xN/GaN HEMTs », *28th International Conference Mixed Design of Integrated Circuits and Systems*, Wroclaw, Poland, June 2020.